Carbon Monoxide Dehydrogenase from *Rhodospirillum rubrum*: Effect of Redox Potential on Catalysis†

Jian Feng‡ and Paul A. Lindahl*,‡,§

Departments of Chemistry and of Biochemistry and Biophysics, Texas A&M University, College Station, Texas 77843-3255

Received September 23, 2003; Revised Manuscript Received December 10, 2003

ABSTRACT: The Ni−Fe−S-containing C-cluster of carbon monoxide dehydrogenases is the active site for catalyzing the reversible oxidation of CO to CO_2. This cluster can be stabilized in redox states designated C_{ox}, C_{red1}, C_{int}, and C_{red2}. What had until recently been the best-supported mechanism of catalysis involves a one-electron reductive activation of C_{ox} to C_{red1} and a catalytic cycle in which the C_{red1} state binds and oxidizes CO, forming C_{red2} and releasing CO_2. Recent experiments cast doubt on this mechanism, as they imply that activation requires reducing the C-cluster to a state more reduced than C_{red1}. In the current study, redox titration and stopped-flow kinetic experiments were performed to assess the previous results and conclusions. Problems in previous methods were identified, and related experiments for which such problems were eliminated or minimized afforded significantly different results. In contrast to the previous study, activation did not correlate with reduction of Fe−S clusters in the enzyme, suggesting that the potential required for activation was milder than that required to reduce these clusters (i.e., $E^0_{act} > -420$ mV vs SHE). Using enzyme preactivated in solutions that were poised at various potentials, lag phases were observed prior to reaching steady-state CO oxidation activities. Fits of the Nernst equation to the corresponding lag-vs-potential plot yielded a midpoint potential of -150 ± 50 mV. This value probably reflects $E^{\circ\prime}$ for the C_{ox}/C_{red1} couple, and it suggests that C_{red1} is indeed active in catalysis.

Nickel-containing carbon monoxide dehydrogenases are found in anaerobic bacteria and archaea, where they catalyze the reversible oxidation of CO to CO_2, reaction 1 (*1*−*3*):

$$CO + H_2O \rightleftarrows CO_2 + 2H^+ + 2\,e^- \qquad (1)$$

Such enzymes found in acetogenic bacteria such as *Moorella thermoacetica* ($CODH_{Mt}$)[1] are bifunctional, with a second active site that catalyzes the synthesis of acetyl-CoA from CO, CoA, and a methylated corrin-iron−sulfur protein. Methanogenic enzymes are also bifunctional and are used for either synthesizing acetyl-CoA or catabolically decomposing acetate (*3*, *4*). Homologues from *Rhodospirillum rubrum* ($CODH_{Rr}$) and *Carboxydothermus hydrogenoformans* ($CODH_{Ch}$) are monofunctional and catalyze only reaction 1. $CODH_{Rr}$ allows *R. rubrum* to grow anaerobically in the dark using CO as a source of energy (*5*, *6*).

X-ray crystal structures of $CODH_{Ch}$, $CODH_{Rr}$, and $CODH_{Mt}$ (from two independent groups) have been published (*7*−*10*). All 4 structures are quite similar, ignoring the α subunits in $CODH_{Mt}$ that are responsible for acetyl-CoA synthesis. CODH portions are β_2 homodimers with molecular masses of 120−140 kDa. Each β subunit contains 1 $\{Ni_{1-}Fe_{4-}S_{4-5}\}$ C-cluster and 1 $[Fe_4S_4]^{2+/1+}$ B-cluster. Another Fe_4S_4 cubane known as the D-cluster bridges the two β subunits. The C-cluster is the active site for CO_2/CO redox (*11*, *12*) and can be viewed as composed of an $[Fe_3S_4]$ cluster linked to a [Ni(S)Fe] unit. The B- and D-clusters transfer electrons between the C-cluster and external redox agents.

Redox and spectroscopic properties of the C-cluster from $CODH_{Mt}$ and $CODH_{Rr}$ have been studied most extensively. Lacking evidence to the contrary, a common set of properties will be assumed for all C-clusters, including stability in four redox states called C_{ox}, C_{red1}, C_{int}, and C_{red2} (Figure 1). The oxidized C_{ox} state is diamagnetic, and probably corresponds to $\{[Ni^{2+}Fe^{3+}]:[Fe_3S_4]^{1-}\}$ (*13*, reinterpreted in ref *1*). After being reduced by one electron ($E^\circ = -110$ mV in $CODH_{Rr}$ (*14*) and −220 mV in $CODH_{Mt}$ (*15*)), it forms an $S = 1/2$ state called C_{red1} and exhibits an EPR signal with $g_{av} = 1.82$ in $CODH_{Mt}$ (*15*, *16*) and $g_{av} = 1.87$ in $CODH_{Rr}$ (*17*,*18*). Mössbauer spectra associated with this transition suggest that C_{red1} can be assigned as $\{[Ni^{2+}Fe^{2+}]:[Fe_3S_4]^{1-}\}$ (*13*, reinterpreted in ref *1*). Further reduction ($E^\circ = -520$ mV at pH 7) causes the C_{red1} signal to disappear and the $S = 1/2$ C_{red2} signal (with $g_{av} = 1.86$) to appear (*13*, *19*). The C_{red2} state is probably two electrons more reduced than C_{red1}, but the site at which the added electrons localize is not known.

In 1994, a mechanism of CO/CO_2 redox catalysis was proposed (*20*) in which CO bound to and was oxidized by

† This work was supported by the National Institutes of Health (Grant GM46441).

* To whom correspondence should be addressed. Phone: (979) 845-0956. Fax: (979) 845-4719. E-mail: Lindahl@mail.chem.tamu.edu.

‡ Department of Chemistry.

§ Department of Biochemistry and Biophysics.

[1] Abbreviations: CODH, carbon monoxide dehydrogenase; $CODH_{Rr}$, CODH from *Rhodospirillum rubrum*; $CODH_{Mt}$, CODH from *Moorella thermoacetica*; $CODH_{Ch}$, CODH from *Carboxydothermus hydrogenoformans*; EPR, electron paramagnetic resonance; MCD, magnetic circular dichroism; MV, methyl viologen; IC, indigo carmine; SHE, standard hydrogen electrode; B_{ox}/B_{red}, oxidized/reduced states of the B-cluster; C_{ox}, C_{red1}, C_{int}, and C_{red}, redox states of the C-cluster, from most oxidized to most reduced; D_{ox}/D_{red}, oxidized/reduced states of the D-cluster.

10.1021/bi0357199 CCC: $27.50
Published on Web 01/24/2004

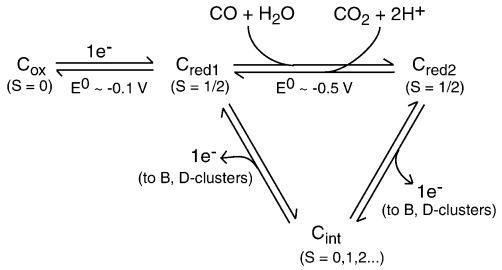

FIGURE 1: Mechanism of CO/CO_2 redox catalysis by CODH's emphasizing redox states of the C-cluster. Details are given in the text.

the C_{red1} state, and in which CO_2 bound to and was reduced by the C_{red2} state, as summarized in reaction 2:

$$CO + H_2O + [C_{red1}]^{n+} \rightleftarrows CO_2 + [C_{red2}]^{(n-2)+} + 2H^+ \quad (2)$$

Later studies (*7*−*13*, *21*, *22*) expanded and embellished this mechanism, affording what will be called the standard mechanism (abbreviated in Figure 1). Accordingly, oxidized C-clusters in the C_{ox} state must be reduced to the C_{red1} state before the enzyme becomes active. CO binds to the Ni of C_{red1} and is attacked by an hydroxyl group bound to the unique Fe in the [Ni Fe] subsite. CO_2 and a proton dissociate, affording C_{red2}. Two electrons are transferred from C_{red2} to external electron acceptors, typically methyl viologen (MV) in vitro. Electrons are transferred one at a time via the B- and D-clusters, traversing an EPR-silent intermediate state called C_{int} (*22*).

There is a lag phase prior to the onset of steady-state CO oxidation by $CODH_{Rr}$ with lengths of 50−150 s, depending on [CO] and [$CODH_{Rr}$] (*23*). Dependence on [$CODH_{Rr}$] indicates that activation is autocatalytic, while the need for CO suggests that active CO-reduced $CODH_{Rr}$ molecules can reduce some site on inactive $CODH_{Rr}$ molecules. Reduction-dependent activation is congruent with the standard mechanism, but the potential at which activation was concluded to occur ($E_m{}^{\circ\prime} = -316$ mV vs SHE) is not. The activation event assumed by the standard mechanism (i.e., $C_{ox} \rightarrow C_{red1}$) occurs with $E^{\circ\prime}$ between −110 and −220 mV, depending on the particular CODH. An alternative interpretation concluded that C_{red1} cannot be the state to which CO binds and is reduced, and that a more reduced state performed this function (*23*, *24*). This interpretation challenges the standard mechanism, as there is no superficial way to make it compatible with this result; an unobserved C-cluster state one-electron more reduced than C_{red2} would be required to retain the fundamental aspects of the standard mechanism.

In this study, these previous experiments (*23*) have been analyzed, and an attempt has been made to reproduce them using a somewhat different approach. Results differ significantly and suggest that the C_{red1} state is indeed the state to which CO binds and reacts. Current results are compared and contrasted to those obtained previously and attempts are made to rationalize differences. Implications for the mechanism of catalysis are discussed.

EXPERIMENTAL PROCEDURES

Growth of R. rubrum. Two-hundred milliliters of media A (6 g/L yeast extract (Fisher), 2 mM $MgSO_4$ (Sigma), 0.7 mM $CaCl_2$ (Sigma), 16 μM ferric citrate (Sigma), 4.5 μM H_3BO_3 (Sigma), 4 μM Na_2MoO_4 (Sigma), 10 μM $NiCl_2$ (Sigma), 1 ng/L Biotin (Sigma), 54 μM EDTA (Sigma), 15 mM Malic Acid (Sigma), 60 mM Phosphate buffer, and 18.7 μM NH_4Cl (Sigma) adjusted to pH 7.0−7.2 and autoclaved at 121 °C for 20 min) in a clear 500 mL Erlenmeyer flask were inoculated with a culture of *R. rubrum* (ATCC: 11170). The flask was placed in a transparent jar whose atmosphere was then replaced with N_2. The culture was exposed for 3 days at room temperature to radiation from 4 × 50-Watt Halogen lights (Sylvania, OSRAM Sylvania Products Inc.) located 1 m away. The culture was transferred into a glass bioreactor containing 25 L media A at 30 °C pre-flushed with N_2. The reactor was exposed to radiation from 14 × 50-Watt Halogen lights located ∼30 cm away. After 4 days of bubbling with N_2, the optical density of the culture at 600 nm reached 3. Lights and N_2 flow were turned off, and the culture was bubbled with CO for 1 day to induce $CODH_{Rr}$ production. The temperature of the bioreactor was chilled to 4 °C, and the culture was transferred into a Coy Box (Model 77, Coy Laboratory Products Inc.) containing a CO_2/H_2 atmosphere. Cells were harvested by centrifugation (Sorvall RC 5C Plus) at 11000 × *g*, frozen in liquid N_2, and stored at − 80 °C.

Purification of $CODH_{Rr}$. In an Ar-atmosphere glovebox (Vac/Atm Inc, Hawthorne CA) containing <1 ppm O_2 as monitored by an O_2-analyzer (Teledyne Analytical Instruments, model 310), $CODH_{Rr}$ was purified as described (*5*, *25*), except that the hydroxylapatite column was not used. Protein purity was quantified by scanning Coomassie-Blue-stained SDS−PAGE gels with an AlphaImager 2000 (Alpha Innotech, San Leandro, CA) and was found to be ca. 94%. Protein concentrations were determined by the Biuret method using bovine serum albumin as a standard (*26*). Concentrations in mg/mL were converted into nM by multiplying by the factor $10^6/62$. Purified $CODH_{Rr}$ was concentrated and washed with reductant-free 100 mM pH 7.5 MOPS (buffer A) 4−5 times using a centricon (YM30, Amicon), yielding a residual dithionite concentration of <10 μM. These as-isolated aliquots were frozen in liquid N_2 and thawed as needed for all other experiments.

CO Oxidation Activity. Standard assays were performed anaerobically using a Beckman 640B UV−visible spectrophotometer as described (*27*), except that the assay buffer lacked EDTA and dithionite. Activity assays involved injecting 3−10 μL of $CODH_{Rr}$ into a 1 cm diameter borosilicate glass tube (Fisher) containing 3.0 mL of 10 mM MV in buffer A previously sealed with a rubber septum (which had been stored in the box >1 month), bubbled with 1 atm CO (prepurified grade) on a Schlenk line, and heated to 30° C. After injection, tubes were shaken, inserted into the spectrophometer, and monitored at 578 nm. Specific activities were calculated using $\epsilon_{578} = 9.7$ mM^{-1} cm^{-1}, path length = 1 cm, and a β-subunit molecular mass of 62 000 Da. The four batches of enzyme purified had specific activities of 1210, 1350, 1020, and 1610 μmol CO oxidized per mg CODH per min (units/mg).

Stopped-Flow Experiments. These were performed anaerobically using a HI-TECH Scientific SF-61 DX2 stopped-flow system in an MBraun LabMaster 130 glovebox containing an Ar atmosphere with <1 ppm O_2 (similarly monitored). Assay buffer was transferred into a drive syringe using an adapter consisting of PEEK tubing terminating in

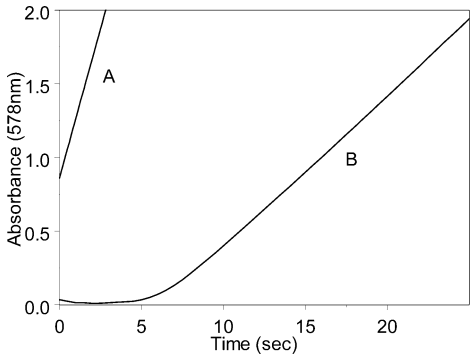

FIGURE 2: CO oxidation activity of $CODH_{Rr}$ as-isolated (A) and after treatment with 100 mM thionin (B). See Experimental Procedures for details. Specific activities for A and B were 810 and 16 units/mg, respectively, as calculated from the linear regions in these traces and taking into account differences in [$CODH_{Rr}$] used.

a Luer connector and needle on one end and a finger-tight connector mounted onto the drive-syringe. After flushing the system with the assay buffer by pulling buffer through the needle, the headspace was eliminated such that the concentration of CO in the assay buffer would match that in the drive syringe. For single-mixing experiments, protein was loaded into a second drive syringe. Final concentrations of protein, redox dyes (MV/IC), and CO were 1/2 of those in the corresponding stock solutions and in the syringe. For double-mixing mode, activation solution in a drive-syringe was mixed with the protein solution in the first mixing step. After an aging time, the resulting solution was mixed with assay solution contained in another driving-syringe. Thus, final concentrations of protein and activation solution were 1/4 of their stock concentrations while final concentrations of assay redox dyes and CO were 1/2 of their stock concentrations.

Activity of Thionin-Treated vs As-Isolated $CODH_{Rr}$. As-isolated $CODH_{Rr}$ (600 μL of 63 μM) was loaded on a DEAE column (0.5 × 7 cm) equilibrated in buffer A and then oxidized by passing 100 mM thionin in buffer A through the column for 5−10 min. Thionin was eluted by passing buffer A through the column until no blue color was evident in the eluent. Thionin-oxidized $CODH_{Rr}$ was then eluted with 0.5 M NaCl in buffer A. The protein was concentrated and washed in a 50 kDa centricon (YM-50, Amicon) until the final concentration of NaCl was < 0.02 M. Thionin-oxidized protein (230 nM, final concentration) and as-isolated $CODH_{Rr}$ (23 nM, final) were assayed for activity as described above (results shown in Figure 2).

Effect of $CODH_{Rr}$ Activation Solution Potential on Lag in CO Oxidation Activity. Aliquots of as-isolated $CODH_{Rr}$ (36 nM, concentration after mixing) were mixed with 3.0 mL of buffer A containing IC (10 μM, final concentration) and variable volumes (0.1 to 10 μL) of 1 mM sodium dithionite (Aldrich). Portions (0.8 mL) of the resulting solutions were loaded into a stopped-flow drive-syringe and incubated for 45−90 min. IC (1.0 mM, final concentration) and CO (440 μM, final concentration) in buffer A were loaded into another drive syringe, and the two solutions were mixed by stopped-flow and monitored in PDA mode (path length, 0.15 cm, 25 °C). At 613 nm, $\Delta\epsilon_{IC} = \epsilon_{oxidized\ IC} - \epsilon_{reduced\ IC} = 25.4\ mM^{-1}\ cm^{-1}$. Within 2 min of completing each stopped-flow experiment, residual protein solutions were removed from the drive syringe and transferred to 1.5 mL Eppendorf tubes that had degassed in the box for ~1 month. The electrochemical potential of each solution was immediately measured in the box using an Accumet Basic AB15 pH meter (Fisher Scientific), an Ag/AgCl reference electrode (MI-401, Micro Electrodes Inc.) and an Au wire (0.127 mm diameter, Aldrich). Electrodes had been stored in the box for more than 2 days before use and calibrated by titrating an anaerobic solution of IC with dithionite. For calibration, measured potentials were plotted against volume of dithionite added, and the potential at the midpoint was assigned to be −125 mV versus SHE ($E^{\circ\prime}$ for the IC couple) (*28*).

RESULTS

The objective of the current study was similar to that of a previous one (*23*), namely, to determine which redox states of the C-cluster are involved in catalysis. In the previous study, $CODH_{Rr}$ samples were oxidized with thionin ($E^{\circ\prime}$ = +64 mV) and then injected into buffered solutions containing different [CO]. In some experiments, rates at which A_{420}-sensitive Fe−S clusters in the enzyme reduced were measured. In other experiments, MV was included in the CO-containing buffer, and rates of MV^{2+}-reduction were measured. In both cases, lag periods prior to the onset of Fe−S or MV^{2+} reduction were measured. "A_{420}-sensitive Fe−S clusters" include the B-cluster, but there is some uncertainty as to whether the C- and D-clusters exhibit redox-sensitive absorbance changes at 420 nm, hence usage of this empirical/operational term. In $CODH_{Mt}$, C_{ox}/C_{red1} and C_{red1}/C_{red2} transitions were reported not to contribute substantially to optical changes in this region (*29*−*31*), while the C_{ox}/C_{red1} transition in $CODH_{Rr}$ appears to be associated with substantial changes at 420 nm (*14*). A reinterpretation of published Mössbauer spectra of Ni-deficient $CODH_{Rr}$ (*13*, *1*) suggests that the D-cluster is redox active with properties similar to those of the B-cluster, while a recent MCD study (*32*) suggests that the D-cluster is redox-inactive and in the $S = 0$ $[Fe_4S_4]^{2+}$ state at all potentials ≥ = −530 mV versus SHE. In this report, redox-active D-clusters will be assumed.

Effect of Thionin on CO Oxidation Activity. A very high concentration of thionin−namely, 100 mM−had been used to oxidize $CODH_{Rr}$ samples in the previous study (*23*). Given that far lower concentrations of thionin irreversibly inactivate $CODH_{Mt}$ (*29*) and give rise to MCD features suggesting C-cluster decomposition products in $CODH_{Rr}$ (*32*), such treatment might have damaged samples. Using what was essentially the previous method of preparation, current thionin-oxidized $CODH_{Rr}$ samples exhibited only 2.5% of the activity of a native $CODH_{Rr}$ control (compare traces A and B in Figure 2). Based on the linear region of the spectral trace in Figure 1A of the previous study (*23*), specific activities between ~0.2 and 1.1 units/mg can be estimated. Such values correspond to orders-of-magnitude less than the typical specific activity of native $CODH_{Rr}$ reported by that lab (1100 (*17*), 4200 (*33*), 4800 (*13*) 6450 (*34*), and 7600 (*27*)). Thus, samples of the previous study appear to have been largely inactive relative to as-isolated $CODH_{Rr}$ prepared previously in the same lab. Low activities may have been caused by damage incurred by oxidation with thionin at inordinately high concentrations.

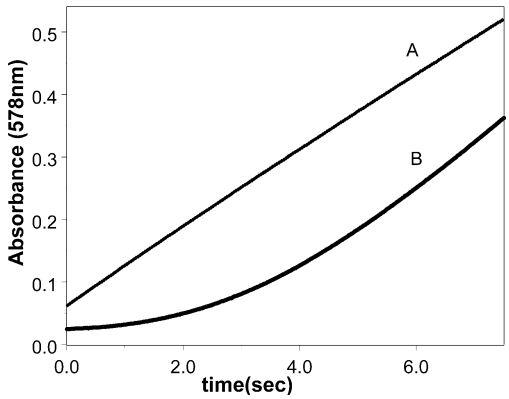

FIGURE 3: Effect of preactivation on CO oxidation activities. (A) As-isolated $CODH_{Rr}$ was mixed with buffer A containing 20 μM MV^{2+} and 20 μM dithionite (concentrations refer to after this mixing step). The solution was aged for 10 s and then mixed with assay buffer containing 10 mM MV and 82 μM [CO] (concentrations after mixing). (B) As-isolated $CODH_{Rr}$ mixed with the same assay buffer as in A but without an activation step. Stopped-flow was performed in PM mode at 578 nm. Protein concentration for samples A and B was 7.7 nM after all mixing steps.

Lag in CO Oxidation Activity. Thionin-oxidized $CODH_{Rr}$ exhibited ~5 s lag phases prior to the onset of CO oxidation activity (Figure 2B). These lags were qualitatively similar to but substantially shorter than the 1−2 min lags reported previously (*23*). Such quantitative differences are consistent with there being a lower proportion of active enzyme in the previous samples, in that the process that abolishes these lags is autocatalytic and thus small changes in $CODH_{Rr}$ concentration would have substantial effects on lag times.

Interpreting lags is quite difficult given that two distinct processes, namely, activation and catalysis, occur concurrently in the experiment just described as well as in analogous experiments previously reported (*23*). Activation involves reducing some site on inactive $CODH_{Rr}$, while catalysis involves active $CODH_{Rr}$ catalyzing reaction 1. By injecting inactive $CODH_{Rr}$ directly in assay buffer and then monitoring formation of product (i.e., MV^{1+}), the observed rate could reflect one or both processes, depending on relative rates. A more easily interpretable experiment would be to activate $CODH_{Rr}$ in one step and measure catalytic activity in another. In this way, sufficient time could be allowed for activation to reach completion, so that the resulting initial catalytic rates could simply reflect the concentration of active enzyme present at the moment of injection.

Using this preactivation method, it became immediately apparent that lags could be eliminated by activating enzyme with either dithionite or dithionite-reduced MV. In a double-mixing stopped-flow experiment, as-isolated $CODH_{Rr}$ was activated for 10 s with a solution of 20 μM MV ($[MV^{1+}]$ = 12 μM; $[MV^{2+}]$ = 8 μM, as determined from A_{578}) and then reacted with CO oxidation buffer. As shown in Figure 3A, the enzyme was fully activated by this procedure. The trace using as-isolated $CODH_{Rr}$ without preactivation exhibited a short lag (Figure 3B), suggesting that such samples are essentially devoid of reductant (the as-isolated sample used to generate the trace in Figure 2A exhibited no lag because the assay solution was manually mixed).

This experiment suggests that small molecules such as dithionite or MV are able to rapidly reduce the activation site on the enzyme, which we presume to be the C-cluster. CO by itself activates the enzyme quite slowly, suggesting that it reduces the activation site indirectly. This could occur by having CO reduce the C-cluster in an active $CODH_{Rr}$ molecule and then having that cluster reduce the B- and D-clusters in the same molecule, which in turn reduces the B- and D-clusters of an inactive $CODH_{Rr}$ molecule, which finally reduces the C-cluster in that molecule. Activation is probably slow because of the lengthy and complex electron-transfer pathway employed.

Rate of Fe−S Cluster Reduction and $CODH_{Rr}$ Activation. CO oxidation activity was previously concluded to be proportional to the fraction of reduced A_{420}-sensitive Fe−S clusters (*23*). This conclusion was based on experiments where the redox potentials of assay solutions were varied, and activity and Fe−S cluster redox status were both measured. Since activation presumably means reducing the C-cluster rather than the B- or D-clusters, the conclusion implies that the active state of the C-cluster is achieved at potentials comparable to $E^{\circ\prime}_{Box/Bred}$ (and probably to $E^{\circ\prime}_{Dox/Dred}$), namely, ca. −418 mV (*35*). Most significantly, this experiment appears to rule out C_{red1} as being the active state of the C-cluster, as $E^{\circ\prime}_{Cox/Cred1} = -110$ mV (*14*).

To reexamine this issue experimentally, thionin-oxidized $CODH_{Rr}$ (prepared using 7.5 mM rather than 100 mM thionin) was reacted with a solution of dithionite and monitored by stopped-flow at 419 nm (Figure 4, I). The A_{420}-sensitive Fe−S clusters in $CODH_{Rr}$ required ~50 s for full reduction under the conditions employed. Immediately thereafter, a double-mixing experiment was performed in which $CODH_{Rr}$ from the same solution that was reduced by dithionite for 1 s and then reacted with CO assay solution and monitored for CO oxidation activity. According to the results just presented, this amount of time would have been sufficient to reduce just 5% of A_{420}-sensitive Fe−S clusters. However, as shown in solid line III of Figure 4, CO was oxidized without a lag phase under these conditions. In contrast, thionin-oxidized $CODH_{Rr}$ that had been mixed with CO assay buffer without being preactivated with dithionite exhibited a ~1 s lag phase. These experiments indicate that dithionite activates $CODH_{Rr}$ in about 1 s and that the enzyme's A_{420}-sensitive Fe−S clusters need not be reduced. This result is consistent with the conclusion that activation involves reduction of C_{ox} to C_{red1} and with the report suggesting that the C_{ox}-to-C_{red1} reduction does not involve a substantial change in absorbance in the 420 nm region (*29*).

Redox Dependence of Lag. In previous experiments, CO oxidation assay solutions were poised at various electrochemical potentials by adding 100 μM (final concentration) redox dyes and adjusting potentials to between −50 and −500 mV using dithionite (*23*). Rates of dye or Fe−S cluster reduction were then measured 5.0 to 5.1 s after adding 0.5 μM thionin-oxidized $CODH_{Rr}$. Rates were normalized to the maximal rates observed, and the resulting "fraction of active enzyme" was plotted versus potential. The Nernst equation was fitted to both plots combined, yielding a midpoint potential of −316 mV ± 8 mV and $n = 1.0 \pm 0.2$ electrons/mol.

Besides using enzyme that was largely inactive and a protocol that did not separate the process of activation from that of catalysis, the thermodynamic driving force for reaction 1 could have been different for each of the experiments used

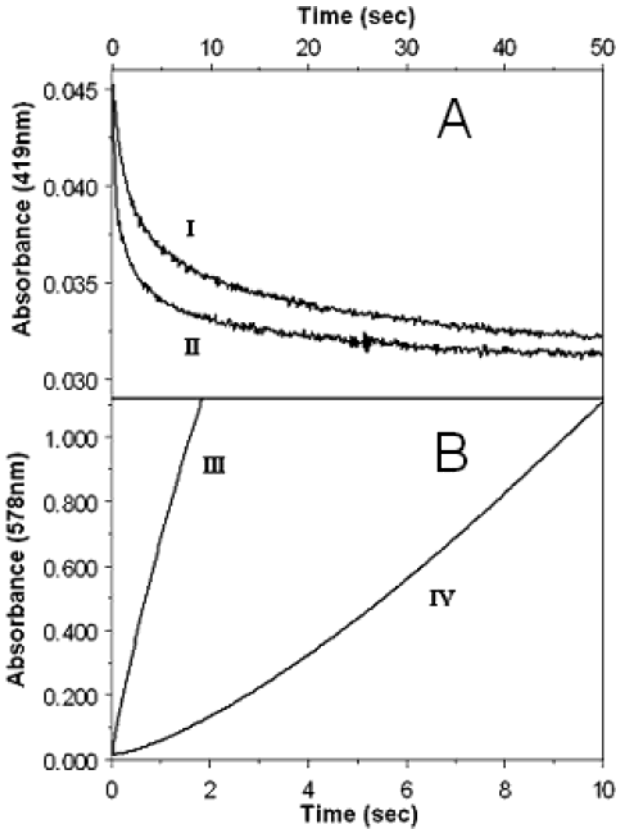

FIGURE 4: Kinetics of A_{420}-sensitive Fe−S cluster reduction. As-isolated $CODH_{Rr}$ was treated with 7.5 mM thionin as described in Experimental Procedures. Panel A: aliquots of this thionin-oxidized sample (3.5 μM) were mixed by stopped-flow at 30 °C with buffer A plus 10 μM (trace I) and 500 μM (trace II) dithionite. Panel B: An aliquot of thionin-oxidized $CODH_{Rr}$ (1.7 μM) was mixed with buffer A containing 10 μM dithionite, and 1 s later with assay solution containing 110 μM CO and 10 mM MV (trace III). Initial activity was 97 units/mg. Another aliquot of this thionin-oxidized $CODH_{Rr}$ (1.7 μM) was mixed with the same assay buffer (trace IV) without prior mixing with dithionite. Traces in panels A and B were monitored in PM mode at 419 and 578 nm, respectively. All concentrations given refer to their final values after all mixing steps.

to generate these plots. For example, the solution poised at −500 mV would have had a much lower driving force than the one poised at −50 mV. This would be so because in the solution poised at −500 mV, $[MV^{1+}]$ would be ≈90% of $[MV]_{tot}$ while $[MV^{2+}]$ would be ≈10% of $[MV]_{tot}$. For the solution poised at −50 mV, $[MV^{1+}]$ would be ≈0, while $[MV^{2+}]$ would be ≈$[MV]_{tot}$. As a result, observed differences in rates at different potentials would not solely reflect differences in the fraction of active enzyme (as assumed) but would also reflect differences in driving force. Correcting for this would lower the calculated $E_{m'}$ for the activation site to values < −316 mV.

To illustrate this effect, dithionite was added to standard CO oxidation assay solution, and the solution potential was estimated from the resulting absorbance due to MV^{1+}. As-isolated $CODH_{Rr}$ was injected, and initial steady-state rates were determined. Values of normalized activity are plotted versus solution potential in Figure 5. The midpoint potential of ∼ −433 mV is near $E^{\circ\prime}$ for MV^{2+}/MV^{1+} couple (−440 mV). Observed activities declined as solution potentials were lowered, yielding a midpoint potential reflecting the E° for the electron acceptor used. In the analogous plot reported previously, activities increased as potentials were lowered

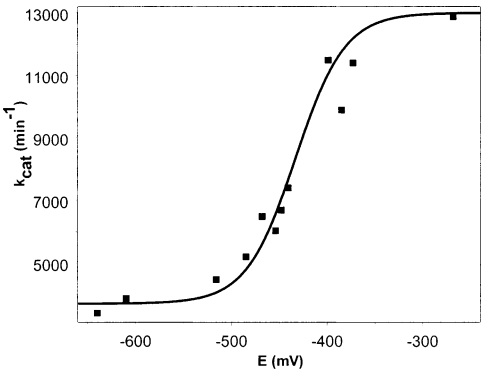

FIGURE 5: Redox-potential dependence of CO oxidation activity without a separate activation step. Variable volumes of 50 mM dithionite (ranging from 0 to 6 μL) were added to 3.0 mL aliquots of 100 mM MOPS, pH 7.5 plus 0.1 mM MV. After 10 min, solutions were bubbled with 1 atm CO and incubated at 30° C. As-isolated $CODH_{Rr}$ (1.5 nM final concentration) was injected, and A_{578} was monitored. Electrochemical potentials of these assay solutions (E) were calculated using the Nernst equation, $[MV^{1+}]$ as determined by UV−vis before injecting enzyme and the relationship $[MV^{2+}] = [MV]_{tot} - [MV^{1+}]$. The fractional activity of a given sample was defined as $Y = (Act - Act_{min})/(Act_{max} - Act_{min})$ where $Act_{max} = 210$ units/mg and $Act_{min} = 60$ units/mg. Fitting the Nernst equation to the resulting Y-vs-E plot yielded best-fit $E^{\circ\prime} = -433$ mV.

(*23*). This behavior is difficult to explain, assuming that the experiment was performed as described.

A similar experiment was performed using a protocol in which $CODH_{Rr}$ samples were incubated for 30 min in activation solutions poised at various potentials before they were injected into CO oxidation assay solutions. In this way, ample time was allowed for the redox state of samples to equilibrate before activities were determined. Uniform assay solutions were also used, so that differences in observed initial rates would simply reflect differences in the concentration of active $CODH_{Rr}$ at the time of injection. Any lags observed would indicate that the potential used in the associated activation step was insufficient to fully activate the enzyme. The length of those lags would equal the time required for enzyme poised as a particular potential to become fully active. Presumably this time is proportional to the extent of the activation reaction that must be completed for enzyme to be fully active.

After preliminary studies using various redox dyes, IC was found to have the redox potential closest to that of the activation couple in $CODH_{Rr}$. Thus, IC was used as a redox buffer in the activation step and as an electron acceptor in the catalysis step. Lags were in fact observed, with lengths that depended on the potential of the activation solution (Figure 6). Lag times were estimated by extrapolating a line through the linear region of these curves and then measuring the times at which those lines intersected the abscissa. Resulting times were plotted versus potential (Figure 7). The Nernst equation assuming (a) $n = 1$, (b) a maximum lag of 3.4 s, and (c) a minimum lag of 0 s was fitted to these data, yielding $E^{\circ} = -150$ mV ± 50 mV vs SHE.

DISCUSSION

Activation of $CODH_{Rr}$. The focus of the current study was to examine previously reported experiments and conclusions that conflicted with the standard mechanism (*23*). For if C_{int}

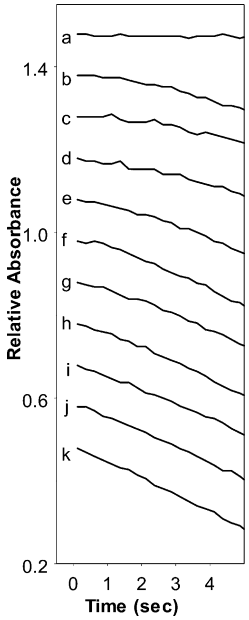

FIGURE 6: Effect of $CODH_{Rr}$ activation solution potential on lag in CO oxidation activity. Aliquots of as-isolated $CODH_{Rr}$ were activated at various potentials and then assessed for CO oxidation activity. See Experimental Procedures for details. Traces at 613 nm are presented with imposed separations of 0.1 absorbance units at the first time point. Potentials of the activation solutions were as follows: b, −28 mV; c, −49 mV; d, −81 mV; e, −116 mV; f, −133 mV; g, −154 mV; h, −228 mV; i, −238 mV; j, −250 mV; k, −255 mV. Trace a is identical to the others, except that no $CODH_{Rr}$ or dithionite was included; the resulting potential was −162 mV.

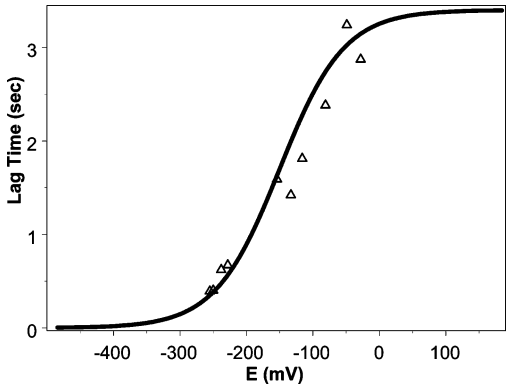

FIGURE 7: Plot of lag time vs potential of activation solution. For each trace in Figure 6 (except trace a), rates and lag times were individually assessed from the slope of the linear region. For traces b−d, this region occurred between 10 and 15 s; for traces e−i, it occurred between 7.5 and 12.5 s; and for traces j and k, it occurred between 5 and 10 s. Rates were calculated from these slopes, while lag times required calculating corresponding horizontal lines from the initial data points of a given trace. The best-fit line thought the linear region of the data was extrapolated to where it intersected the horizontal line. The lag was defined as the time interval from $t = 0$ to that point. The Nernst equation was fitted to the resulting plot of lag times vs potentials of the activation solution.

is the state to which CO binds and is oxidized, as was concluded, another C-cluster state two electrons more reduced than it must be used to bind and reduce CO_2. This is so because the enzyme operates reversibly and CO and CO_2 differ in redox state by two electrons (literally by an oxygen atom). However, there is no known state of the C-cluster two-electrons more reduced than C_{int}. This dilemma could be resolved by reassigning previous redox and spectroscopic states, but this could not be done in a manner that was physically realistic and justified by the data. Also, doing so now seems unnecessary, as previous results which cast doubt upon the standard mechanism are themselves somewhat in doubt. Current experiments found that thionin irreversibly inactivates $CODH_{Rr}$, with longer exposure and higher concentrations resulting in greater damage; the previous study used this oxidant at inordinately high concentrations. An experimental protocol was also employed that did not separate the process of activation from catalysis; as a result, observed rates are not easily interpretable. In previous experiments where redox potentials of assay solutions were adjusted from sample to sample, the thermodynamic driving force for assay determinations might have varied as well, again obscuring analysis.

The current study used as-isolated $CODH_{Rr}$ in a preactivation protocol where enzyme was first activated (to different degrees) and then assayed for catalytic activity. In this manner, the resulting initial activities reflected the concentration of active enzyme at the time of injection, while any lag observed reflected the extent to which activation had not been completed in the first step.

These differences in sample preparation and experimental design may be responsible for the different results obtained. Specifically, reduction of Fe−S clusters was found not to be directly correlated to the activity of the enzyme. Rather, $CODH_{Rr}$ was fully active even when a large proportion of its A_{420}-sensitive Fe−S clusters were oxidized. The only redox couple of the C-cluster having a reduction potential greater than those of the B-cluster ($E^{\circ\prime}_{Box/Bred} \approx -418$ mV) and probably D-cluster is C_{ox}/C_{red1} ($E^{\circ\prime}_{Cox/Cred1} = -110$ mV). Thus, this result is consistent with the conclusion that reducing C_{ox} to C_{red1} activates oxidized enzyme and is inconsistent with the previous conclusion (*23*) that a more reduced redox couple of the C-cluster serves this function. The best-fit $E^{\circ\prime}$ obtained from the data of Figure 7 also supports the conclusion that activation results from reducing C_{ox} to C_{red1}. The ∼40 mV difference between the value obtained in this study and $E^{\circ}_{Cox/Cred1}$ is within the uncertainties of the two determinations. Moreover, there is no other C-cluster couple that is closer to the calculated value (e.g., $E^{\circ}_{Cred1/Cred2} = -520$ mV for $CODH_{Mt}$).

Why the value for the activation potential as calculated in this study differed by over 160 mV from that calculated previously (*23*) could not be satisfactorily explained. A different type of activation process may have been measured previously, involving species on $CODH_{Rr}$ that must be reduced before C_{ox}, B_{ox} or D_{ox} could be reduced. Consider a redox-dependent conformational change involving Active (Act) and Inactive (Inact) states, with properties shown below:

$$\text{CODH}\{\text{Act: } C_{any};B_{any};D_{any}\} + \text{Thionin} \rightarrow \text{CODH}\{\text{Inac: } C_{ox};B_{ox};D_{ox}\} \quad E_{ox} \approx +100 \text{ mV}$$

$$\text{CODH}\{\text{Inact: } C_{ox};B_{ox};D_{ox}\} + \text{ne}^- \rightarrow \text{CODH}\{\text{Act: } C_{red};B_{red};D_{red}\} \quad E_{red} \approx -418 \text{ mV}$$

$$\text{CODH}\{\text{Act: } C_{ox};B_{ox};D_{ox}] + 1\text{e}^- \rightleftarrows \text{CODH}\{\text{Act: } C_{red1};B_{ox};D_{ox}\} \quad E^0_{Cox/Cred1} = -110 \text{ mV}$$

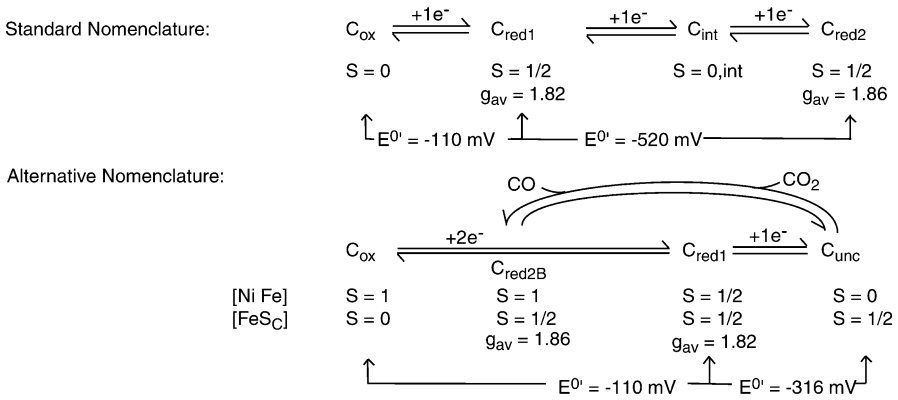

FIGURE 8: Comparative schemes for C-cluster redox states. See text for details.

Consider that thionin oxidizes the enzyme into the Inact conformation, and that this conformation that can only be reduced to the Act conformation at potentials of ca. −418 mV. In other words, the redox process would be hysteretic. A value of −418 mV rather than the measured −316 mV has been assumed for the reductive conversion back to the Act conformation so as to match $E^{\circ\prime}_{Box/Bred}$. Consider further that the C-cluster could be reduced (for kinetic reasons, not for thermodynamic ones) from the C_{ox} to C_{red1} state only after the enzyme was in its *Act* conformation. This model explains how Fe−S clusters (with $E^{\circ\prime}_{Box/Bred} \approx E^{\circ\prime}_{Dox/Dred} \approx$ −418 mV) and the C-cluster in the C_{ox} state (with $E^{\circ\prime}_{Cox/Cred1}$ = −110 mV) could have both been reduced at the same potential as observed (*23*).

Differences in Nomenclature and Proposed Mechanisms. Differences between the standard mechanism outlined in Figure 1 and the alternative mechanism (most clearly illustrated in Figure 2 of *24*) is summarized in Figure 8. The alternative mechanism treats the two subcomponents of the C-cluster {[Ni (S) Fe] and [Fe_3S_4]} as separate entities that weakly spin-couple with each other and/or with the B_{red} cluster in various redox states (*36*, *37*). Fully oxidized C-cluster (i.e., C_{ox}) is assigned as {[$(CO_L)Fe^{2+}$−Ni^{2+}]$^{4+}$ $S = 1$ and FeS_C^{2+} $S = 0$}. Two-electron reduction yields a state assigned as {[$(CO_L)Fe^{3+}$−Ni^{2+}−H^-]$^{4+}$ $S = 1/2$ and FeS_C^{1+} $S = 1/2$} and called C_{red1}. C_{red1} is presumed to be a spin-coupled integer-spin state that gives rise to the g_{av} = 1.82 EPR signal and is thus similar to the C_{red1} state of the standard mechanism in terms of EPR signal and reduction potential. However, the C_{red1} of the alternative mechanism (to be called C_{red1}-alt) is one electron further reduced relative to C_{ox}. The most reduced C-cluster state of the alternative mechanism, called C_{unc}, is 1-electron further reduced than C_{red1}-alt. This "uncoupled" EPR-silent C-cluster state has been assigned as {[$(CO_L)Fe^{2+}$-Ni^{2+}-H^-]$^{3+}$ $S = 0$ and FeS_C^{1+} $S = 1/2$} and has been equated to the C_{int} state of the standard mechanism. Again this correspondence is correct in terms of EPR signal (or lack thereof, in this case) and arguably reduction potential, but not in terms of oxidation state (C_{unc} is 1-electron more reduced than C_{int}). Upon treatment with CO_2, C_{unc} is thought to convert to an $S = 1/2$ state called C_{red2B} which exhibits the $g_{av} = 1.86$ signal (this signal arises from the fully reduced C_{red2} state of the standard mechanism). According to the alternative mechanism (Figure 2, *23*)

$$CO + H_2O + [C_{red2B}]^{n+} \rightleftarrows CO_2 + [C_{unc}]^{(n-2)+} + 2H^+ \quad (3)$$

Thus, C_{red2B} is viewed as being two electrons more oxidized than C_{unc}, which places it between C_{ox} and C_{red1}-alt (Figure 8). Reactions 3 and 2 are equivalent except for a name change in C-cluster states. However, differences are not merely semantic, as the CO-oxidizing state of the standard mechanism (C_{red1}) develops with $E^{\circ\prime} = -110$ mV while that for the alternative mechanism (C_{red2B}) develops with $E^{\circ\prime} = -316$ mV. C_{red2B} is considered to be more reduced than C_{red1} (*23*), but a comparative electron count shows that it is actually isoelectronic with the C_{red1} and one electron more oxidized than C_{red1}-alt. This leads to an "inversion" of redox states in which C_{red2B} is proposed to develop with a lower redox potential than C_{red1} even though it is more oxidized. Also, C_{red2B} (the state yielding the $g_{av} = 1.86$ signal) is viewed as developing only in the presence of CO_2, but the $g_{av} = 1.86$ signal can be generated in the absence of CO_2 (*13*, *15*, *16*, *19*, *20*, *22*, *30*). This leads to a predicted order for the appearance of C-cluster EPR signals (as oxidized CODH is titrated with reductants in the absence of CO_2) that is not observed. The alternative model seems to predict the initial development of the $g_{av} = 1.86$ signal, as C_{ox} converts to C_{red2B}, followed by the rise of the $g_{av} = 1.82$ signal (using g-values for $CODH_{Mt}$) as C_{red2B} converts to C_{red1} with concomitant decline of $g_{av} = 1.86$, ultimately forming an EPR-silent situation as C_{red1} converts to C_{unc}. Experimentally, the $g_{av} = 1.82$ signal develops first, followed by its decline and corresponding development of the $g_{av} = 1.86$ signal; the EPR-silent C_{int} state is only evidenced under nonstandard and very specific conditions (*22*). Finally, the spectroscopic assignment of the C_{red1} state as a spin-coupled integer state (*36*, *37*) has been criticized (*1*) as incompatible with Mössbauer spectra of this state (*13*). These spectra show magnetic hyperfine interactions in the absence of a magnetic field, indicative of a half-integer spin state. Taken together, these problems suggest that the alternative mechanism should be reconsidered.

REFERENCES

1. Lindahl, P. A. (2002) *Biochemistry 41*, 2097−2105.
2. Fontecilla-Camps, J. C., and Ragsdale, S. W. (1999) *Adv. Inorg. Chem. 47*, 283−333.
3. Ferry, J. G. (1995) *Annu. Rev. Microbiol. 49*, 305−333.
4. Lindahl, P. A., and Chang, B. (2001) *Origins Life Evolution Biosphere 31*, 403−434.

5. Bonam, D.; Murrell, S. A., and Ludden, P. W. (1984) *J. Bacteriol. 159*, 693−699.
6. Kerby, R. L., Ludden, P. W., and Roberts, G. P. (1995) *J. Bacteriol. 177*, 2241−2244.
7. Dobbek H., Svetlitchnyi, V., Gremer, L., Huber, R., and Meyer, O. (2001) *Science 293*, 1281−1285.
8. Drennan, C. L., Heo, J., Sintchak, M. D., Schreiter, E., and Ludden, P. W. (2001) *Proc. Natl. Acad. Sci. U.S.A. 98*, 11973−11978.
9. Doukov, T. L., Iverson, T. M., Seravalli, J., Ragsdale, S. W., and Drennan, C. L. (2002) *Science 298*, 567−572.
10. Darnault, C, Volbeda, A, Kim, E. J., Legrand, P., Vernede, X., Lindahl, P. A., and Fontecilla-Camps, J. C. (2003) *Nat. Struct. Biol. 10*, 271−279.
11. Anderson, M. E., DeRose, V. J., Hoffman, B. M., and Lindahl, P. A. (1993) *J. Am. Chem. Soc. 115*, 12204−12205.
12. Seravalli, J., Kumar, M., Lu, W. P., and Ragsdale, S. W. (1995), *Biochemistry 34*, 7879−7888.
13. Hu, Z., Spangler, N. J., Anderson, M. E., Xia, J., Ludden, P. W., Lindahl, P. A., and Münck, E. (1996) *J. Am. Chem. Soc. 118*, 830−845.
14. Spangler, N. J., Lindahl, P. A., Bandarian, V., and Ludden P. W. (1996) *J. Biol. Chem. 271*, 7973−7977.
15. Lindahl, P. A., Münck, E., and Ragsdale, S. W. (1990) *J. Biol. Chem. 265*, 3873−3879.
16. Lindahl, P. A., Ragsdale, S. W., and Münck, E.(1990) *J. Biol. Chem. 265*, 3880−3888.
17. Bonam, D., and Ludden, P. W. (1987) *J. Biol. Chem. 262*, 2980−2987.
18. Stephens, P. J., McKenna, M. C., Ensign, S. A., Bonam, D., and Ludden, P. W. (1989) *J. Biol. Chem. 264*, 16347−16350.
19. Russell, W. K., and Lindahl, P. A. (1998) *Biochemistry 37*, 10016−10026.
20. Anderson, M. E., and Lindahl, P. A. (1994) *Biochemistry 33*, 8702−8711.
21. DeRose, V. J., Anderson, M. E., Lindahl, P. A., and Hoffman, B. M.(1998) *J. Am. Chem. Soc. 120*, 8767−8776.
22. Fraser, D. M., and Lindahl, P. A. (1999), *Biochemistry 38*, 15706−15711.
23. Heo, J., Halbleib, C. M., and Ludden, P. W. (2001), *Proc. Natl. Acad. Sci. U.S.A. 98*, 7690−7693.
24. Heo, J., Staples, C. R., and Ludden, P. W. (2001) *Biochemistry 40*, 7604−7611.
25. Heo J., and Ludden, P. W. (1999) *J. Am. Chem. Soc. 121*, 11034−11044.
26. Pelley, J. W., Garner, C. W., and Little, G. H. (1978) *Anal. Biochem. 86*, 341−343.
27. Ensign, S. A., Hyman, M. R., and Ludden, P. W. (1989) *Biochemistry 28*, 4973−4979.
28. Srividya, N., Paramasivan, G., Seetharaman, K., and Ramamurthy, P. (1994) *J. Chem. Soc., Faraday Trans. 90*, 2525−2530.
29. Shin, W., Stafford, P. R., and Lindahl, P. A. (1992) *Biochemistry 31*, 6003−6011.
30. Anderson, M. E., and Lindahl, P. A. (1996) *Biochemistry 35*, 8371−8380.
31. Seravalli, J., Kumar, M., Lu, W. P., and Ragsdale, S. W. (1997) *Biochemistry 36*, 11241−11251.
32. Craft, J. L., Ludden, P. W., and Brunold, T. C. (2002) *Biochemistry 41*, 1681−1688.
33. Ensign, S. A., and Ludden, P. W. (1991) *J. Biol. Chem. 266*, 18395−18403.
34. Heo, J., Staples, C. R., Halbleib, C. M., and Ludden, P. W. (2000) *Biochemistry 39*, 7956−7963.
35. Smith, E. T., Ensign, S. A., Ludden, P. W., and Feinberg, B. A. (1992) *Biochem. J. 285*, 181−185.
36. Staples, C. R., Heo, J., Spangler, N. J., Kerby, R. L., Roberts, G. P., and Ludden, P. W. (1999), *J. Am. Chem. Soc. 121*, 11034−11044.
37. Heo, J., Staples, C. R., Telser, J., and Ludden, P. W. (1999) *J. Am. Chem. Soc. 121*, 11045−11057.

BI0357199